Journal of Invertebrate Pathology 199 (2023) 107948

Contents lists available at ScienceDirect

Journal of Invertebrate Pathology

journal homepage: www.elsevier.com/locate/jip

Alternosema astaquatica n. sp. (Microsporidia: Enterocytozoonida), a systemic parasite of the crayfish *Faxonius virilis*

Cheyenne E. Stratton [a,*], Lindsey S. Reisinger [a], Donald C. Behringer [a,b], Aaron W. Reinke [c], Jamie Bojko [d,e,*]

[a] *Fisheries and Aquatic Sciences, University of Florida, Gainesville, FL 32653, USA*
[b] *Emerging Pathogens Institute, University of Florida, Gainesville, FL 32611, USA*
[c] *Department of Molecular Genetics, University of Toronto, Toronto, Ontario, Canada*
[d] *School of Health and Life Sciences, Teesside University, Middlesbrough TS1 3BX, UK*
[e] *National Horizons Centre, Teesside University, Darlington DL1 1HG, UK*

ARTICLE INFO

Keywords:
Freshwater
Parasite
Histopathology
Orthosomella
Pancytospora
Opisthosporidia

ABSTRACT

Crayfish have strong ecological impacts in freshwater systems, yet our knowledge of their parasites is limited. This study describes the first systemic microsporidium (infects multiple tissue types) *Alternosema astaquatica* n. sp. (Enterocytozoonida) isolated from a crayfish host, *Faxonius virilis*, using histopathology, transmission electron microscopy, gene sequencing, and phylogenetics. The parasite develops in direct contact with the host cell cytoplasm producing mature spores that are monokaryotic and ellipsoid in shape. Spores have 9–10 coils of the polar filament and measure 3.07 ± 0.26 μm (SD) in length and 0.93 ± 0.08 μm (SD) in width. Our novel isolate has high genetic similarity to *Alternosema bostrichidis* isolated from terrestrial beetles; however, genetic data from this parasite is restricted to a small fragment (396 bp) of the SSU gene. Additional data related to spore morphology and development, host, environment, and ecology indicate that our novel isolate is distinct from *A. bostrichidis,* which supports a new species description. *Alternosema astaquatica* n. sp. represents a novel member of the *Orthosomella*-like group which appears to be a set of opportunists within the Enterocytozoonida. The presence of this microsporidium in *F. virilis* could be relevant for freshwater ecosystems across this crayfish's broad geographic range in North America and may affect interactions between *F. virilis* and invasive rusty crayfish *Faxonius rusticus* in the Midwest USA.

1. Introduction

Microsporidia are a group of obligate, intracellular parasites that infect a diversity of hosts (Murareanu et al. 2021). Traditionally, microsporidian systematics included a series of clades; however, an updated phylogenetic framework has introduced a classical naming system, based most importantly on genetic/genomic information, with supporting morphological, ultrastructural, developmental, and ecological data (Wijayawardene et al. 2020; Bojko et al. 2022). These higher taxonomic units consist of the Amblyosporida, Caudosporida, Glugeida, Nosematida, Ovavesiculida, Neopereziida, and the Enterocytozoonida. Microsporidia from the Enterocytozoonida group are found in freshwater, marine, and terrestrial hosts and in a range of host taxa (Stentiford et al. 2019; Bojko et al. 2022).

Enterocytozoonida members tend to infect the crustacean hepatopancreas (Stentiford et al. 2011; Bojko et al. 2017; Bojko et al. 2023a), but their diversity and broad tissue tropism include members that infect the gonad, epidermis, and gut (Bojko et al. 2022). In most Crustacea, tissue tropism can help to identify microsporidian species; however, in crayfish, there is a broad diversity of microsporidian pathogens from all corners of the phylogeny (Bojko et al. 2020a; Stratton et al. 2022a). To date, nine microsporidian species have been formally described from, or associated with, crayfish hosts globally (Moodie et al., 2003a; Moodie et al., 2003b; Moodie et al., 2003c; Pretto et al., 2018; Bojko et al., 2020a; Bojko et al., 2020b; Tokarev et al. 2020; Stratton et al., 2022a; Stratton et al. 2022b). These include the genera: *Cambaraspora*, *Ovipleistophora*, *Nosema* (previously *Vairimorpha*), and *Astathelohania*.

Early observations of microsporidian infections in crayfish led to terms like "porcelain disease", due to parasite accumulation in the host

* Corresponding authors.
E-mail addresses: c.stratton@ufl.edu (C.E. Stratton), J.Bojko@tees.ac.uk (J. Bojko).

https://doi.org/10.1016/j.jip.2023.107948
Received 7 April 2023; Received in revised form 24 May 2023; Accepted 31 May 2023
Available online 3 June 2023

muscle tissue, which becomes opaque in heavily infected individuals (Freeman et al., 2010). Muscle-infecting microsporidia usually cause a loss of muscle function, and can ultimately result in death (Freeman et al., 2010). For example, *Astathelohania* (orphan lineage), *Ovipleistophora* (Glugeida), and *Nosema* spp. (Nosematida) have all been found to infect crayfish muscle tissue, but they all come from different taxonomic orders in the Rozellomycota (Microsporidia) (Bojko et al. 2022).

Systemic microsporidiosis (infection in multiple tissue types) in crayfish is relatively rare, and to date, no formally described species induces systemic infection in a crayfish. In this study, we describe *Alternosema astaquatica* n. sp., a novel member of the Enterocytozoonida which presents as a systemic infection in multiple host organs of *Faxonius virilis*. This novel microsporidium is the first member of the Enterocytozoonida identified from a crayfish. We explore this parasite and its interactions with its host using histopathology, transmission electron microscopy (TEM), gene sequencing, and phylogenetics.

2. Materials and methods

2.1. Sample collection

All crayfish were collected from two lakes in Vilas County, Wisconsin, USA using baited minnow traps. Twenty-six individuals were collected from Horsehead Lake (45.784764, −89.585641) on the 1st of July 2019. Twenty-one individuals were collected from Van Vliet Lake (46.192112, −89.754363) on the 5th of July 2019. Animals were stored in lake water during transport to Trout Lake Station, Vilas County, Wisconsin.

2.2. Histology

Crayfish were examined for gross signs of microsporidian infection (white abdominal muscle tissue) and then anaesthetized by being placed on ice for 10 min prior to dissection. For histopathological screening, crayfish were dissected to obtain tissue biopsies of muscle, eye, antennal gland, gill, nerve, heart, gonad, hepatopancreas, and gut, which were placed into a plastic cassette. Tissue cassettes were submerged in Davidson's Freshwater Fixative (tap water, ethanol, formaldehyde, glacial acetic acid) for 48 h and then transferred to 70% ethanol (Bojko et al. 2020a; Stratton et al. 2022a). The ethanol-fixed tissues were then dehydrated and underwent a xylene exchange prior to infiltration with paraffin wax and embedding into wax blocks. Wax blocks were sectioned with a microtome, producing 3–4 μm thick sections, which were floated on a water bath (~40 °C) with 2 ml of Sta-on (Leica). These sections were mounted on glass slides and allowed to dry on a hot plate set at ~ 50 °C. The slides were then dewaxed (xylene – ethanol - water), dehydrated, and stained with haematoxylin and alcoholic eosin. A cover-slip was then placed onto each slide. Slides were screened using a Leica DM500 microscope. Images of histology slides were captured using a Leica camera.

2.3. Electron microscopy

During dissection, biopsies of the antennal gland, hepatopancreas, gill, and muscle tissue were fixed in 2.5% glutaraldehyde in a 0.1% sodium cacodylate buffer for transmission electron microscopy (TEM) (Bojko et al. 2020a; Stratton et al. 2022a). Antennal gland tissue infected with the microsporidium was transferred to 4% paraformaldehyde with 2.5% glutaraldehyde in 0.1 M sodium cacodylate (pH 7.24). A Pelco BioWave Pro laboratory microwave (Ted Pella, Redding, CA, USA) was used to process fixed tissues. The samples were secondarily fixed in 2% osmium tetroxide after a 0.1 M sodium cacodylate (pH 7.24) wash. The sample then underwent a water wash followed by dehydration in a graded ethanol series (25% to 100% in 5–10% increments) and finally 100% acetone. The dehydrated sample was resin infiltrated using an ARALDITE/Embed epoxy resin and Z6040 embedding primer (Electron Microscopy Services (EMS), Hatfield, PA). Samples were infiltrated with 100% ARAKDITE/Embed after infiltration of anhydrous acetone: ARALDITE/Embed in increments of 3:1, 1:1, and 1:3.

The resin-infiltrated sample was cut into semi-thin sections (500 nm) after curing for 72 h at 60 °C and then stained with toluidine blue. These sections were then cut ultra-thin and collected on carbon-coated Formvar 100 mesh grid (EMS, Hatfield, PA) and stained with lead citrate ($C_{12}H_{10}O_{14}Pb_3$) and 2% aqueous uranyl acetate [$UO_2(CH_3COO)_2$] (EMS, Hatfield, PA). A FEI Teenai G2 Spirit Twin TEM (FEI Corp., Hillsboro, OR) was used to view the stained ultra-thin sections. A Gatan UltraScan 2 k × 2 k camera with Digital Micrograph software (Gatan Inc., Pleasanton, CA) was used to capture digital images of sections and ImageJ software was used to take morphology measurements of TEM images (Schneider et al. 2012).

2.4. PCR diagnostics

Biopsies of the antennal gland, muscle, hepatopancreas, and gill tissue were fixed in 96% molecular-grade ethanol for molecular diagnostics. Each of these tissues underwent DNA extraction using Qiagen's DNeasy Blood and Tissue Kit (qiagen.com) following the manufacturer's protocol. Each tissue type required a different length of time for the Proteinase K to digest before becoming completely lysed. Muscle tissue was digested for 5 h, antennal glands were digested for 1 h, gill tissue was digested for 2 h, and hepatopancreas tissue was digested for 30 min. Extracted DNA was used in a 50 μl reaction Promega 'FlexiTag PCR (promega.com) consisting of 0.25 μl of Promega Taq polymerase, 10 μl buffer, 0.5 μl dNTPs, 5 μl $MgCl_2$, 0.5 μl forward primer V1F (5′-CACCAGGTTGATTCTGCCTGAC-3′) and 0.5 μl reverse primer 530r (5′-CCGCGGCTGCTGGCAC-3′) (Vossbrinck et al., 1993; Baker et al., 1994). Thermocycler conditions were a 94 °C initial denaturation for 3 min then 30 cycles of 94 °C denaturation for 30 s, 58 °C annealing for 30 s, and a 72 °C elongation period for 30 s followed by a 10-minute final extension period at 72 °C. Amplicons were visualized on a 1.5% agarose gel using gel electrophoresis. The resulting microsporidian-specific amplicon was ~ 400 bp. A gel extraction was performed on bands excised from a gel using Qiagen's gel extraction kit (qiagen.com). Samples were sent for forward and reverse sequencing to Eurofins Genomics (eurofinsgenomics.com).

2.5. Metagenomics and sequence annotation

The antennal gland of one infected animal was sent for metagenomic sequencing. DNA extraction was conducted as described above and the sample was shipped on dry ice to Novogene (USA), who produced the TruSeq DNA library and sequenced the library on a HiSeq X platform. The resulting dataset included 2,152,970 forward and 2,371,070 reverse raw reads. The raw data were trimmed using Trimmomatic v.0.39 (parameters: leading: 3, trailing: 3, sliding window: 4:15, minlen:36) (Bolger et al. 2014). The trimmed data were uploaded to the Kaiju webserver (https://kaiju.binf.ku.dk/server) (parameters: NCBI BLAST *nr* + *euk* (2022–03-10), greedy mode, mml: 11, mms: 75, allowed mismatches: 5, max. e-value: 0.0001) (Menzel et al. 2016). Kaiju determined that an estimated 184,388 reads (<1.9% of the total reads) were associated with the Microsporidia (Fig. 1). The trimmed dataset was assembled using SPAdes v.3.15.3 (Bankevich et al. 2012) (parameters: phred-offset 33), and resulted in 265,123 contiguous sequences > 500 bp. Quast v.5.0.2 (Gurevich et al. 2013) identified the following statistics based on assembly quality: N50: 819, L50: 89,142. Metaxa2 (v.2.1.3) was used on the assembled data to determine which contig included the microsporidian SSU (length: 5,226 bp, coverage: 33.5X) (NCBI accession: OM501730). The SSU sequence was compared to existing sequences on NCBI using BLASTn.

The contiguous sequences were subject to a bespoke BLASTx screen, with a protein database developed from the predicted proteins of two *Pancytospora* genomes (NCBI accessions: JALRLY010000000;

Fig. 1. Kaiju output used to determine the approximate number of trimmed reads associated with the Microsporidia. In this case, microsporidian genomes for *Astathelohania (=Thelohania) contejeani*, *Enterospora canceri*, and others, are the closest available comparisons from the web server output (data availability: *nr* + euk, database date: 2022–03-10) that associate with the sequence data available for *Alternosema astaquatica* n. sp. and other contaminating sequences (e.g. host sequences) that make up the metagenomic dataset.

JALRLY000000000). Microsporidian sequences (e-value < 1.0e-100) were pulled from the original contigs and then annotated using GeneMarkS (Besemer et al. 2001; parameters: 'intronless eukaryotic', genetic code: 11). BUSCO v.5.3.0 (Seppey et al. 2019; parameters: Microsporidiaodb10-(05/08/2020)) was used to determine the microsporidian genome completeness. The annotated proteins from the new isolate were analysed using OrthoFinder (Emms and Kelly, 2019) alongside the two *Pancytospora* spp. genomes (see above) to determine single gene orthologues between these *Orthosomella*-like group microsporidia. InterProScan v.5.60–92.0 was used to determine the protein family (-appl Pfam) of the hypothetical annotated proteins (Jones et al. 2014). The final genomic segments can be located at NCBI accession: JARRAN000000000.

2.6. Identification of proteins belonging to nematode-infecting microsporidia large gene families

Proteins from *A. astaquatica* that belong to large-gene families were identified as described in Wadi et al. (2022). First, proteins were predicted from the genome using Prodigal v2.6.3 (Hyatt et al. 2010) with translation Table 1. These predicted proteins were then searched against the 37 nematode-infecting microsporidia large gene family HMM models (NemLGF1-28, PanLGF1-3, and EbrLGF1-6) using the hmmsearch function in HMMER 3.3.2 (Eddy, 2011). All proteins with an e-value cut-off of less than 10–5 are listed in Supplementary Table 1. Signal peptides for these proteins were predicted using SignalP 6.0 (Teufel et al. 2022). To determine the phylogenetic relationship of NemLGF1 proteins we identified these proteins in the genomes of *N. parisii*, *N. major*, *P. epiphaga*, and *P. philotis* using hmmsearch, as described above. Proteins predicted to either be partial or less than 500 amino acids long were excluded. The remaining 241 proteins were aligned with MUSCLE (https://toolkit.tuebingen.mpg.de/tools/muscle) and a maximum likelihood tree was generated using RAxML-NG v.0.9.0 (Kozlov et al. 2019) with 100 bootstraps using model JTT + I + G4 + F as determined by ModelTest-NG v0.1.6 (Darriba et al. 2020).

Table 1
Collection information for each individual crayfish with an indication of the tissue types the microsporidium was observed in during histological screening and detected with PCR diagnostics. Tissue types include: AG = antennal gland; CT = connective tissue; GI = gill; GD = gonad; GU = gut epithelial tissue; HE = heart myocardium; HP = hepatopancreas; MU = skeletal muscle.

Host Species	Site	Coordinates	Collection Date	Sex	Carapace Length (mm)	Histology								PCR Detection			
						AG	CT	GI	GD	GU	HE	HP	MU	AG	GI	HP	MU
F. virilis	Horsehead	46.235031, −89.713187	01 July 2019	F	43	✓	✓	✓	✓	✓	✓	—	✓	✓	—	✓	✓
F. virilis	Van Vliet	46.186643, −89.753253	05 July 2019	MII	20	✓	✓	✓	✓	✓	✓	✓	—	✓	✓	✓	✓
F. virilis	Van Vliet	46.186643, −89.753253	06 July 2019	F	29	✓	—	—	✓	—	—	—	—	✓	✓	✓	✓
F. virilis	Van Vliet	46.186643, −89.753253	06 July 2019	MII	49	✓	✓	✓	—	✓	✓	—	—	✓	✓	✓	✓

2.7. Phylogenetic analysis

The complete SSU sequence derived from the metagenomic data for the new microsporidium was added to a FASTA file, alongside 135 other microsporidian isolates and a *Metchnikovella dogeli* outgroup. The sequences were aligned using MAFFT on the CIPRES gateway (https://www.phylo.org). The aligned file was then submitted to the IQ-TREE web server (https://iqtree.cibiv.univie.ac.at; Trifinopoulos et al. 2016). The analysis was conducted over 2010 columns, including bases and gaps. The appropriate evolutionary model was selected according to Bayesian information criteria to be GTR + F + I + G4. The maximum-likelihood analysis generated a phylogenetic tree, which was run for > 1000 bootstraps and resulted in a final log-likelihood of −64237.443.

3. Results

3.1. Histopathology and ecological prevalence

Two *F. virilis* individuals collected from Van Vliet Lake exhibited gross pathological signs in the form of white spots on internal organs and tissues only visible upon dissection. The prevalence of infection in *F. virilis* collected from Van Vliet Lake was 14.29% (3/21) and 3.85% (1/26) from Horsehead Lake. The size range of *F. virilis* individuals collected from Van Vliet Lake was 20–56 mm carapace length (CL) and the sex

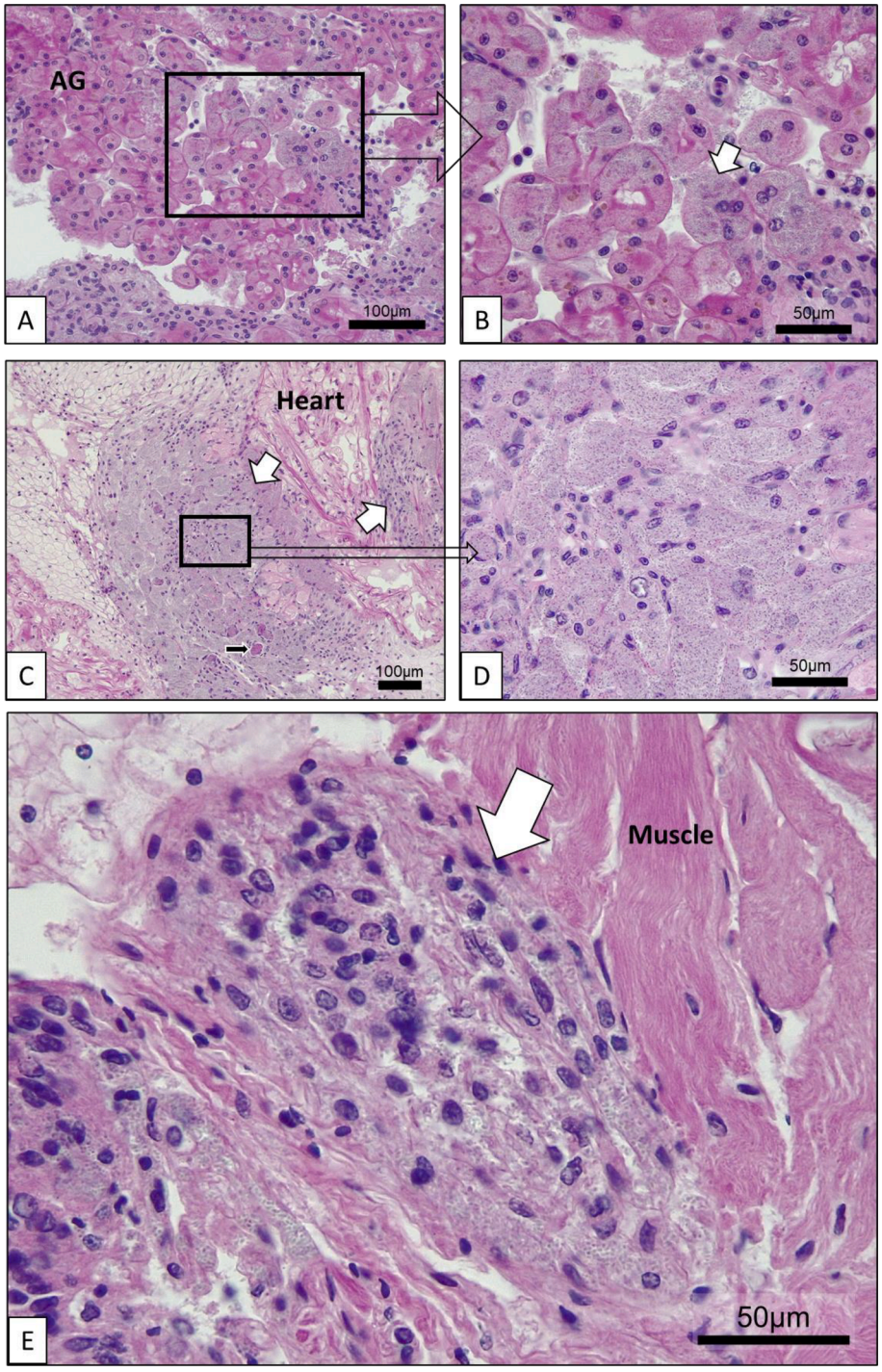

Fig. 2. Microsporidian infection of the antennal gland (AG), heart and muscle tissue of *Faxonius virilis*. (a-b) AG epithelia present a microsporidian infection in the cytoplasm of the cell, exhibiting some cytological hypertrophy. (c-d) Heart myocardium infected by the microsporidium (white arrows), which appears to target the connective tissue primarily. Spores can be seen in the cytoplasm of the infected cells. Melanisation is also visible as an immune response to the infection (black arrow). (e) Infection of the tail muscle was also visible on one small area of the slide (white arrow), with evidence of the muscle fibres and surrounding connective tissue being targeted.

ratio was 9:12 (M:F). The size range in Horsehead Lake was 25–49 mm CL and the sex ratio was 8:18 (M:F). However, only a single female (CL: 43 mm) was infected with the microsporidium.

The histological screening revealed microsporidian spores developing in direct contact within the host cell cytoplasm of various cell types in the antennal gland (Fig. 2a-b), gonad, heart myocardium (Fig. 2c-d), skeletal muscle (Fig. 2e), haemal sinuses of the hepatopancreas, gills, gut epithelial tissue, and connective tissues of the infected individuals – this resulted in an organism-wide systemic pathology (Table 1). Immune responses noted from the histological section were in the form of small patches of melanisation (Fig. 2c).

3.2. Ultrastructure and intracellular lifecycle

The development of this microsporidium occurred in direct contact with the host cytoplasm (overview and development diagram; Fig. 3). Development begins with a putative monokaryotic meront (Fig. 4a). The nucleus divides to form a diplokaryotic meront (Fig. 4b). The diplokaryotic meront divides further to form two monokaryotic sporonts (Fig. 4c). The sporonts further develop into sporoblasts, where the primordial polar filament can be observed (Fig. 4d). The sporont elongates to become oblong in shape, where further development of the polar filament takes place (Fig. 4d-e). The spore became oval in shape as it neared maturity, and the cytoplasm then begins to darken with the production of large numbers of ribosomes (Fig. 4f). Mature spores were monokaryotic and measured 3.07 ± 0.26 μm (n = 5; SD) in length and 0.93 ± 0.08 μm (n = 10; SD) in width (Fig. 4g; Table 2). The spores were oval/ellipsoid in shape once completely developed. The ultrastructure included a posterior vacuole, anchoring disc, bi-laminar polaroplast, and polar filament which coiled 9–10 times with a diameter of 92–112 nm (n = 8) (Fig. 4h-j). The spore had a well-developed spore wall, which included an electron-dense exospore and electron-lucent endospore measuring 23–37 nm (n = 8) and 31–54 nm (n = 8), respectively. The spore wall thinned over the anchoring disc (Fig. 4h).

3.3. Gene sequence data, phylogenetics, and predicted protein function

We sequenced the LSU, ITS and SSU region (5,226 bp) of the novel microsporidium, which was assembled from a metagenomic dataset derived from infected host antennal gland tissue. The SSU region showed the greatest similarity to a short 396 bp SSU fragment from *Alternosema bostrichidis* (KP455651; 99.24% similarity; e-value: 0.0), a microsporidian parasite of a terrestrial beetle. Overall, the complete sequence most closely resembled a 1203 bp SSU fragment from *Percutemincola moriokae* (LC136798; 95.01% similarity; e-value: 0.0). The closest similar sequence to the LSU region of the novel parasite was *Vittaforma corneae* (Enterocytozoonida) (XR_552275; 83.78% similarity; e-value: 5e-78) and *Endoreticulatus* sp. (Enterocytozoonida) (FJ772431; 84.59% similarity; e-value: 6e-77). The SSU-ITS-LSU region was used as a standard in this study to provide taxonomic clarity, following the system suggested in Bojko et al. (2022) and is presented in section 4 of this manuscript (Taxonomic Description).

The maximum-likelihood phylogenetic tree supported that the new crayfish microsporidium sits within the Enterocytozoonida (100% bootstrap confidence) (Fig. 5a). Within the Enterocytozoonida, the Enterocytozoonidae and *Enterocytospora*-like group clade together with strong support (100%; including the 'ultimate opportunists'). The grouping of an *Orthosomella*-like group was also highly supported (100%), and included *Orthosomella operophterae*, *Enteropsectra longa*, and *Liebermannia covasacrae* at the base of this group, followed by a cluster of globally distributed but largely similar (~93–99%) microsporidian isolates which included our novel isolate (Fig. 5b-c). *Percutemincola moriokae* and *Pancytospora epiphaga* form one sub-cluster on the tree, where the novel microsporidian isolate from *F. virilis* is present on the same branch as *A. bostrichidis*. The isolates represented in this sub-cluster of the *Orthosomella*-like group are distributed globally, including isolates from Japan, Russia, Mexico, USA, and Canada, derived from eDNA sampling, nematodes, coleopterans, amphipods, and now decapods.

After metagenomic assembly, the host:parasite raw read ratio (Fig. 1) in the sample was low, restricting our ability to achieve a high-quality genome draft, and leaving us with an average of 3.35X coverage across the genomic contigs (total: 611 contigs; max: 21,070 bp – min: 1,000 bp). Despite the low coverage, GeneMarkS annotation resulted in a total of 1,016 intronless eukaryotic genes being predicted from the draft genome. BUSCO analysis identified the genome draft for the new microsporidium to be ~ 31.4% complete (187 complete, 1 complete and duplicated, and 52 fragmented, out of 600 testable BUSCOs). OrthoFinder analysis (comparing our sequence annotation to the available *Pancytospora* spp. genomes) determined 708 comparable single-copy orthologues between the three genomes, which were further annotated using InterProScan (480 with a determinable Pfam, 228 remain hypothetical). InterProScan determined the protein function of the 480 annotated genes to be spread across 343 Pfam predictions, with 22 Pfams present in 3 or more annotated proteins, highlighting these functional domains as more common in our dataset (Fig. 6; Supplementary Table 2). The most common protein group was PF00069 (protein kinase) – 15 predicted protein kinases were present in *A. astaquatica* as well as *P. epiphaga* and *P. philotis*. Other common Pfams

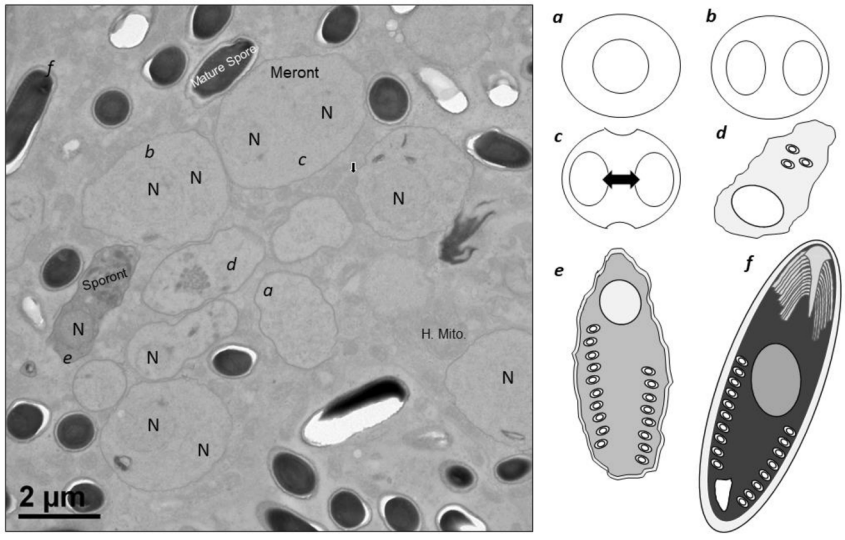

Fig. 3. Developmental stages of *Alternosema astaquatica* n. sp. within the antennal gland of *Faxonius virilis* The TEM photo shows various developmental stages occurring in close proximity to one another in direct contact with host cell cytoplasm. The right illustrates each stage of development including (a) monokaryotic meront, (b) diplokaryotic meront, (c) meront diving to become monokaryotic sporonts, (d) monokaryotic sporont developing organelles, (e) sporoblast, (f) mature monokaryotic spore.

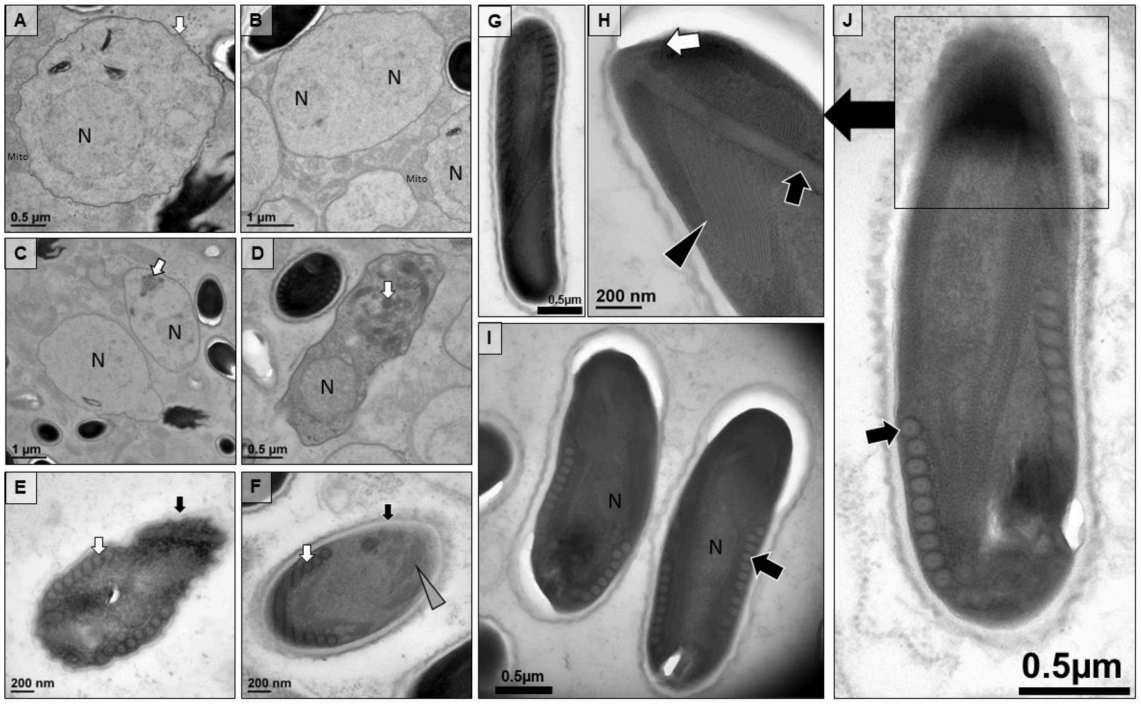

Fig. 4. Development of *Alternosema astaquatica* n. sp. within the antennal gland of *Faxonius virilis.* (a) A putative monokaryotic (N) meront with an electron-dense cell wall (white arrow) developing in direct contact with host mitochondrion. (b) A diplokayotic (N) meront. (c) Unikaryotic (N) sporonts beginning to develop electron-dense organelles (white arrow). (d) Unikaryotic (N) sporoblast developing polar filament (white arrow). (e) Sporoblast with a well-developed polar filament (white arrow) and a thickening spore wall (black arrow). (f) A near mature spores with polar filament (white arrow) and developing spore wall with a thick electron-lucent endospore and electron-dense exospore (black arrow) with ribosome clusters present in an array (gray arrowhead). (g) A mature spore highlighting the elongated ellipsoid shape of the spore. (h) Shows the details of the anchoring disc (white arrow) leading into the polar filament (black arrow) and bilaminar polarplast (black arrowhead). (i) Two monokaryotic (N) mature spores with the polar filament (black arrow) coiled in a single layer. (j) The ultrastructure of a mature spore consists of a polar filament (black arrow), spore wall consisting of electron-denes exospore and electron-lucent endospore, and the details of the anterior of the spore are found in 4 h.

Table 2
Morphological features of the two described *Alternosema* species.

Morphological feature	***A. astaquatica* n. sp.**		***A. bostrichidis*[1]**
Spore Shape	Ellipsoid		Ovoid
Spore length (µm)	3.07 (2.75–3.35)	n = 5	3.8 (3.5–5.0)
Spore width (µm)	0.93 (0.75–1.00)	n = 10	2.5 (2.4–2.8)
No. coils in polar filament	9–11		11–17
Polar filament diameter (nm)	92–112	n = 8	113–122
Lateral exospore thickness (nm)	23–37	n = 8	49–55
Lateral endospore thickness (nm)	31–54	n = 8	190–220

[1] Lipa et al. 2020.

included: structural maintenance of the chromosome (PF00493), helicases (PF00270, PF00271), and general AAA ATPase proteins (PF00004), among others (Fig. 6).

Finally, one group of particular interest are large gene families that have been documented in many microsporidian species (Reinke et al. 2017). Large gene families are especially prominent in nematode-infecting microsporidia. Given the phylogenetic relationship of *A. astaquatica* to *Pancytospora,* we examined the presence of this genome for the 37 families that have been reported from nematode-infecting microsporidia (Wadi et al. 2022). We identified 4 proteins (two full-length) from NemLGF1, two proteins from NemLGF2, and no proteins from any of the other families (Supplementary Table 1). The two proteins from NemLGF2 only contain a RING domain and not the rest of the protein sequence that defines this family, so these proteins are likely not directly evolutionarily related. To determine the phylogenetic relationship of the NemLGF1 proteins, we built a protein family tree containing the sequences from *A. astaquatica* and several *Pancytospora* and *Nematocida* species. The NemLGF1 protein sequences from *A. astaquatica* form a well-supported clade with members from *Pancytospora,* confirming that these proteins share a recent common ancestor (Supplementary Fig. 1).

4. Taxonomic description

4.1. Higher taxonomy

Superphylum: Opisthosporidia Karpov et al. (2014).

Phylum: Rozellomycota (Tedersoo et al. 2018), including Microsporidia (Balbiani, 1882) (Wijayawardene et al. 2020).

Class: Terresporidia Vossbrinck et al. (2014).

Order: Enterocytozoonida Bojko et al. (2022).

Family: *Orthosomella*-like (pending description) (Wijayawardene et al. 2020).

4.2. Genus: Alternosema Lipa, Tokarev and issi (2020)

Description: "*The microsporidium is monoxenous, monomorphic, develops in direct contact with the host cell cytoplasm. Binary fission throughout the life cycle. Two merogonial cycles. The meronts of the first merogony and all the consequent developmental stages are diplokaryotic* or monokaryotic. *The surface of the meront/sporont transitional stage is covered with a thick layer of electron-dense granules – future exospore. Spores are ovoid, with a thick endospore and a two-layered exospore. The latter is composed of granular material and thin electron-translucent structures.*" – amend. (Lipa et al. 2020).

Type host: "Prostephanus truncatus *(Coleoptera, Bostrichidae)*" – (Lipa et al. 2020).

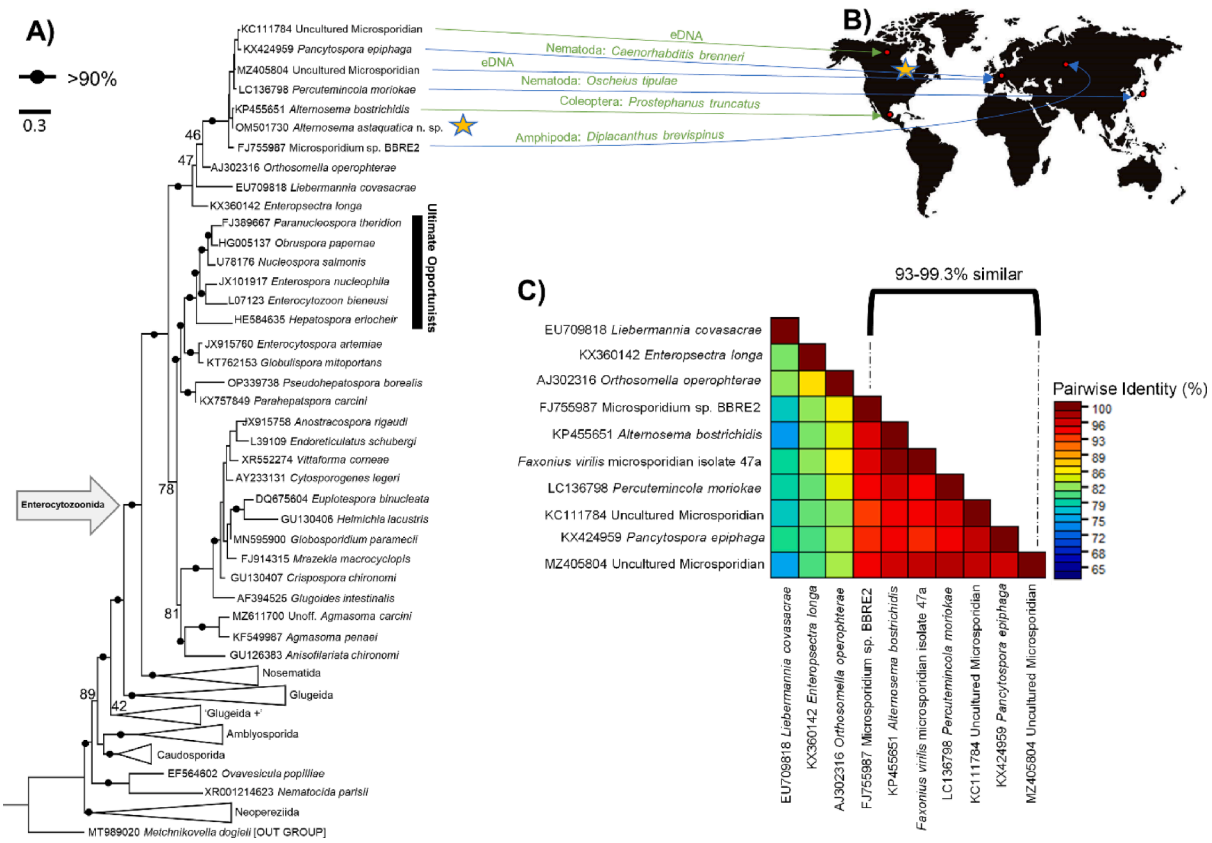

Fig. 5. The phylogenetic placement of *Alternosema astaquatica* n. sp. (a) A maximum-likelihood phylogenetic tree of SSU sequences from microsporidian isolates found in the Enterocytozoonida, compared to other microsporidian groups. The isolate sequenced in this study is indicated by the star on the tree. (b) The annotated map indicates the location each isolate was discovered. The star shows where our isolate was found in Wisconsin, USA. (c) A similarity matrix reflects the percent similarity between microsporidian isolates with > 93% similarity to *Alternosema astaquatica* n. sp. as well as other members of Enterocytozoonida.

Etymology: "*Based on* Nosema *with the prefix Alter-, implying "other"*" – (Lipa et al. 2020).

4.3. Species description and other details

Novel species: *Alternosema astaquatica* n. sp. Stratton, Reisinger, Behringer, Reinke and Bojko, 2023.

Description: Microsporidia within this species should fall between 99 and 100% similarity to the ~ 5 Kb SSU-ITS-LSU gene region sequenced for the type specimen (OM501730). The microsporidium is monoxenous, monomorphic and does not produce a sporophorous vesicle, developing in direct contact with the host cell cytoplasm. Mature spores are monokaryotic. The mature spore shape represents an elongated ellipsoid measuring 3.07 ± 0.26 μm (SD) in length and 0.93 ± 0.08 μm (SD) in width with 9–10 coils of the polar filament.

Type host: *Faxonius virilis* (Cambaridae) Hagen, 1870.

Type locality: Van Vliet Lake (46.192112, −89.754363), Vilas County, Wisconsin, USA.

Site of infection: Antennal gland, connective tissues, gills, gonad, gut epithelial tissue, haemal sinuses of the hepatopancreas, skeletal muscle, and heart myocardium.

Etymology: The species '*astaquatica*' can be split into '*asta*' (Astacoidae) meaning crayfish, and '*aquatica*' meaning aquatic, after the host's habitat.

Type material: Histology slides, resin blocks, and ethanol-fixed tissue are stored at the Reisinger Laboratory, University of Florida. SSU data are reposited in NCBI under accession: OM501730 and genomic data are stored under BioProjects: PRJNA950574 (SRA database) and PRJNA950224; and BioSample: SAMN33980182; genome: JARRAN000000000.

5. Discussion

Crayfish are globally important freshwater animals that often dominate the invertebrate biomass and have strong impacts on freshwater ecosystem community structure and function, making their health status a vitally important topic (Momot, 1995; Rabeni et al. 1995). Through the years, several microsporidian species have been identified from crayfish, including the genera: *Astathelohania*, *Cambaraspora*, *Ovipleistophora*, *Nosema*, and more taxonomically unofficial observations (Longshaw 2011; Bojko et al. 2020a; Stratton et al. 2022a; Stratton et al. 2022b). We add to this growing diversity by providing histological, ultrastructural, developmental, and genetic data for a new species: *Alternosema astaquatica* n. sp. (Enterocytozoonida). This new species is genetically similar to *A. bostrichidis*; however, the genetic data available for this species is restricted to a 396 bp SSU fragment. We explore the geography, host range, and pathology of the *Orthosomella*-like group, as well as what this new microsporidium may mean for a native freshwater crayfish in the lakes within and around Wisconsin, USA.

5.1. The Orthosomella-like group and Alternosema taxonomy

Within the Enterocytozoonida, we see a large range of hosts, microsporidian development pathways, host tissue tropism, and gain/loss of metabolic pathways (Wiredu Boakye et al., 2017; Murareanu et al. 2021; Bojko et al. 2022). This group of Microsporidia infects a range of hosts and houses the "ultimate opportunists" – highly opportunistic parasites of fish, crustaceans, and humans (Stentiford et al. 2019). The known diversity within the Enterocytozoonida has grown, including recent discoveries of crustacean parasites from this systematic order: e.g. *Pseudohepatospora* (Bojko et al. 2023a), *Parahepatospora*

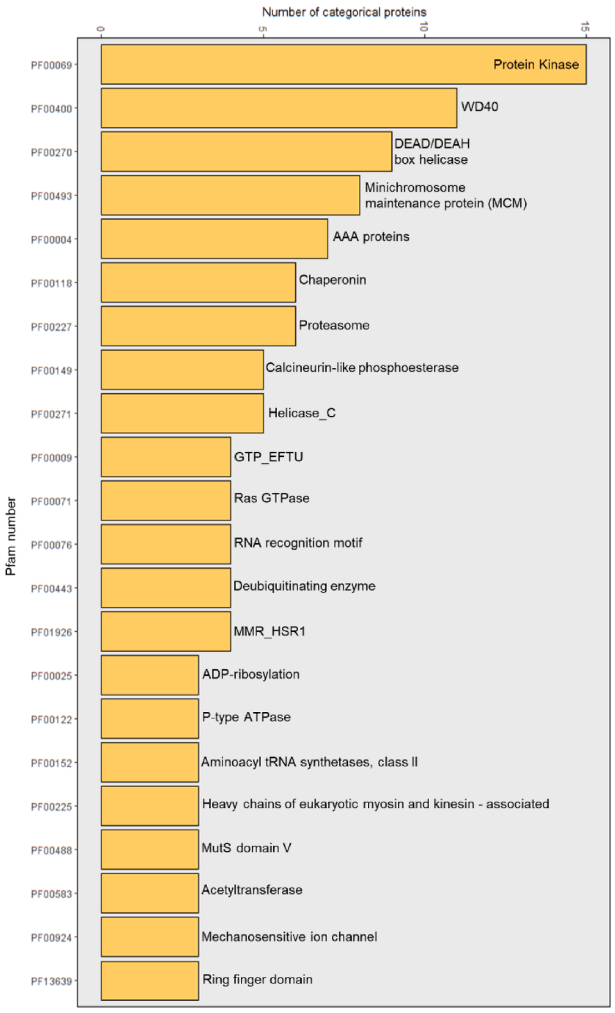

Fig. 6. Pfam domains present in three or more individual proteins across the annotated *Alternosema astaquatica* n. sp. genome. InterProScan was used to determine the Pfam for each protein (Supplementary Table 2), resulting in 22 Pfam domains that were most common (X axis). The general function of the Pfam is listed to the right of the bar. Developed in R v.4.0.3, ggplot2 (Wickham, 2011).

(Bojko et al. 2017), *Globulispora* (Vávra et al., 2016), *Agmasoma* sp. (Sokolova et al., 2015; Frizzera et al., 2021; Bojko et al., 2023b), and several members that compose the ever-growing *Orthosomella*-like group (Dubuffet et al. 2021; Chauvet et al. 2022).

The *Orthosomella*-like group contains the following genera: *Percutemincola*, *Pancytospora* (polyphyletic), *Orthosomella*, *Enteropsectra*, *Liebermannia*, and *Alternosema* (Dubuffet et al. 2021). *Percutemincola moriokae* infects the terrestrial nematode, *Oscheius tipulae* (Nishikori et al. 2018). Two *Pancytospora* spp. (*P. epiphaga* and *P. philotis*) infect the terrestrial nematodes *Oscheius tipulae* and *Caenorhabditis brenneri*, both of which have their genomes sequenced at the draft level (JALRLY010000000; JALRLY000000000; Wadi et al. 2022). *Orthosomella operophterae* infects a terrestrial insect (moth) from the UK, *Operophtera brumata* (Canning et al. 2001). *Enteropsectra longa* infects the terrestrial nematode, *Caenorhabditis elegans*, and *Enteropsectra breve* infects the terrestrial nematode *Oscheius tipulae* (Zhang et al. 2016). *Liebermannia* spp. (*L. covasacrae*; *L. dichroplusae*; and *L. patagonica*) infect terrestrial insects (grasshoppers) from Argentina: *Covasacris pallidinota*, *Dichroplus elongatus*, and *Tristira magellanica* (Sokolova et al. 2006; Sokolova et al. 2007; Lange and Azzaro, 2008). Finally, the two *Alternosema* spp. (*A. bostrichidis* and *A. astaquatica* n. sp.) infect the terrestrial insects (beetles) *Prostephanus truncates* and *Dinoderus* spp. (Lipa et al. 2020) and, in our study, the freshwater crayfish *F. virilis*. Genetic data are available for several other isolates that are also likely members of this group: KC111784 (soil eDNA; Ardila-Garcia et al. 2013), MZ405804 (freshwater eDNA; Dubuffet et al. 2021), and FJ755987 (Amphipoda: *Diplacenthus brevispinus*) (Russia; Lake Baikal).

Orthosomella-like group diversity appears primarily terrestrial and infects invertebrate hosts. Despite being mostly terrestrial, there are three aquatic representatives; one collected using eDNA, one from an amphipod, and ours from a crayfish. Our study is the first to show that a microsporidium in this group causes a systemic pathology in its crustacean host. We also show that, despite the close genetic similarity between *A. bostrichidis* and *A. astaquatica* n. sp. (~99%, over 396 bp; Lipa et al. 2020), which is only over a small available fragment of the *A. bostrichidis* SSU gene, that the two are dissimilar based on spore morphology and development, ecology, host, and environment - all supporting a new species description (Table 2). Greater sequencing of the *A. bostrichidis* genome could help to show us whether this species and *A. astaquatica* are the same, and if they should be considered the same species with morphological plasticity, a broad geographic range, and the capacity to infect crustacean and insect hosts.

Comparative genomics between *A. astaquatica* n. sp. and other Microsporidia is limited by our low coverage sequence data (~3.35X) and partial completeness (BUSCO: 31.4%). However, we were able to annotate 1,016 proteins, 708 of which were shared by the closest available relatives (*Pancytospora* spp.) with high-quality genome drafts (Wadi et al. 2022). The two *Pancytospora* spp. are both nematode-infecting microsporidia, and the most pertinent features of their genomes included the presence of the (*Nematocida* large gene families) NemLGF1 despite their presence in the Enterocytozoonida instead of the Ovavesiculida (Bojko et al. 2022). Wadi et al. (2022) found NemLGF1 proteins associated with *P. philotis* (n = 81) and *P. epiphaga* (n = 45), and here we show that there are two full-length proteins from *A. astaquatica* that are members of the NemLGF1 family. This family is enriched in proteins that contain signal peptides and that are localized inside of *C. elegans* intestinal cells, suggesting that these proteins are used by the parasite to interface with their host (Reinke et al. 2017). As NemLGF1 proteins have only ever been previously detected in nematode-infecting microsporidia, their identification in *A. astaquatica* suggests a useful function for microsporidia infecting other animal phyla. The number of proteins reported for this family ranges from 45 to 231. As only two full-length proteins were observed for *A. astaquatica,* this may mean that this family did not undergo expansion to the same extent as in the nematode-infecting microsporidian species, or that additional members of this family in *A. astaquatica* were missed due to the partially incomplete genome assembly.

Given the broad host range of the *Orthosomella*-like group members, and their high degree of genetic similarity (Fig. 5c), research into this group may be uncovering another set of opportunists within the Enterocytozoonida. Instead of humans, fish, and Crustacea (like the "ultimate opportunists"; Stentiford et al. 2019) that are infected by members of the Enterocytozoonidae, we instead are seeing nematodes, insects and crustaceans infected by members of the *Orthosomella*-like group.

5.2. A systemic microsporidian parasite in a North american crayfish

Faxonius virilis is one of the most widely distributed crayfish species in North America with invasive populations throughout (Taylor et al. 2015; Stratton and DiStefano, 2021). It is native to the midwestern USA including Vilas County, WI (Taylor et al. 2015). In this region, the invasive rusty crayfish (*Faxonius rusticus*) outcompetes *F. virilis* for habitat and resources and often becomes the most dominant crayfish species in invaded waterbodies (Olden et al. 2006). To date, little is known about the parasite community harboured by *F. virilis* outside of the recently described *Astathelohania virili* found in the same region (Stratton et al. 2022a). Due to the propensity of Microsporidia to decrease host fitness, the presence of this parasite in a native species

could put them at a competitive disadvantage to the invasive *F. rusticus* (Freeman et al. 2010, Lipa et al. 2020). In both lakes where we found *A. astaquatica*, *F. rusticus* has invaded and the *F. virilis* populations have subsequently moved to less desirable habitats (e.g., mucky habitat with macrophytes), supporting our hypothesis that they are being outcompeted. Moreover, this shift in habitat may alter the parasites they are exposed to and further decrease their competitive ability.

5.3. Conclusion

Due to the ecological importance of freshwater crayfish, it is vital to know what parasites may impact their health and fitness. Here we provide a formal description of the first systemic microsporidium from a crayfish host, *Alternosema astaquatica* n. sp., in the *Orthosomella*-like group (Enterocytozoonida). This finding provides evidence of another group of opportunist Microsporidia within the Enterocytozoonida as supported by the broad host range yet high genetic similarity of the *Orthosomella*-like group – in particular, *A. bostrichidis* from a Mexican coleopteran and *A. astaquatica* from a freshwater crayfish. The detection of some Nem family proteins encoded by this new microsporidian may indicate the potential for transfer between nematodes or could alternatively represent remnants of genome evolution of *A. astaquatica*, perhaps due to co-evolving with nematode hosts.

If this microsporidium alters *F. virilis* abundance or its relative competitive ability, it is likely to have substantial consequences for the lake community structure and ecosystem function across infected populations.

Declaration of Competing Interest

The authors declare that they have no known competing financial interests or personal relationships that could have appeared to influence the work reported in this paper.

Acknowledgements

Thanks to Emily An and Natalie Stephens for assistance with the collection of crayfish and to Nicole Machi at the Electron Microscopy Core (University of Florida, Interdisciplinary Centre for Biotechnology Research, RRID: SCR_019146) for their work on these pathogens. Funding for this research was provided by the Wisconsin Department of Natural Resources to LSR, DCB and JB (AIRD11519).

Appendix A. Supplementary data

Supplementary data to this article can be found online at https://doi.org/10.1016/j.jip.2023.107948.

References

Ardila-Garcia, A.M., Raghuram, N., Sihota, P., Naomi, M.F., 2013. Microsporidian diversity in soil, sand, and compost of the Pacific Northwest. J. Eukaryot. Microbiol. 60 (6), 601–608.

Baker, M.D., Vossbrinck, C.R., Maddox, J.V., Undeen, A.H., 1994. Phylogenetic relationships among *Vairimorpha* and *Nosema* species (Microspora) based on ribosomal RNA sequence data. J. Invertebr. Pathol. 30, 509–518.

Balbiani, E., 1882. Sur Les Microsporidies Ou Psorospermies Des Articules. Compt. Rend. Acad. Sco Paris. 95, 1168–1171.

Bankevich, A., Nurk, S., Antipov, D., Gurevich, A.A., Dvorkin, M., Kulikov, A.S., Pevzner, P.A., 2012. SPAdes: a new genome assembly algorithm and its applications to single-cell sequencing. J. Comput. Biol. 19 (5), 455–477.

Besemer, J., Lomsadze, A., Borodovsky, M., 2001. GeneMarkS: a self-training method for prediction of gene starts in microbial genomes. Implications for finding sequence motifs in regulatory regions. Nucleic Acids Res. 29, 2607–2618.

Bojko, J., Clark, F., Bass, D., Dunn, A.M., Stewart-Clark, S., Stebbing, P.D., Stentiford, G. D., 2017. *Parahepatospora carcini* n. gen., n. sp., a parasite of invasive *Carcinus maenas* with intermediate features of sporogony between the Enterocytozoon clade and other Microsporidia. J. Invertebr. Pathol. 143, 124–134.

Bojko, J., Behringer, D.C., Moler, P., Reisinger, L., 2020a. *Ovipleistophora diplostomuri*, a parasite of fish and their trematodes, also infects the crayfish *Procambarus bivvittatus*. J. Invertebr. Pathol. 169, 107306.

Bojko, J., Behringer, D.C., Moler, P., Stratton, C.E.L., Reisinger, L., 2020b. A new lineage of crayfish-infecting Microsporidia: The *Cambaraspora floridanus* n. gen. n. sp. (Glugeida: Glugeidae) complex from Floridian freshwaters (USA). J. Invertebr. Pathol. 171, 107345.

Bojko, J., Reinke, A.W., Stentiford, G.D., Williams, B., Rogers, M.S., Bass, D., 2022. Microsporidia: a new taxonomic, evolutionary, and ecological synthesis. Trends Parasitol. 38, 642–659.

Bojko, J., Behringer, D.C., Bateman, K.S., Stentiford, G.D., Clark, F.P., 2023a. *Pseudohepatospora borealis* n. gen. n. sp. (Microsporidia: Enterocytozoonida): a microsporidian pathogen of the Jonah crab (*Cancer borealis*). J. Invertebr. Pathol. 107886.

Bojko, J., Frizzera, A., Vázquez, N., Taylor, G., Rand, V., Cremonte, F., 2023b. Comparative genomics for *Agmasoma* sp. (Microsporidia) parasitising invasive *Carcinus aestuarii* and *Carcinus maenas* in Argentina. J. Invertebr. Pathol. 107908.

Bolger, A.M., Lohse, M., Usadel, B., 2014. Trimmomatic: a flexible trimmer for Illumina sequence data. Bioinformatics 30 (15), 2114–2120.

Canning, E.U., Curry, A., Cheney, S.A., Lafranchi-Tristem, N.J., Ebert, D., Rifardt, D., Killick-Kendrick, R., 2001. *Flabelliforma montana* (Phylum Microsporidia) from *Phlebotomus ariasi* (Diptera, Psychodidae): ultrastructural observations and phylogenetic relationships. Eur. J. Protistol. 37 (2), 207–221.

Chauvet, M., Debroas, D., Moné, A., Dubuffet, A., Lepère, C., 2022. Temporal variations of Microsporidia diversity and discovery of new host–parasite interactions in a lake ecosystem. Environ. Microbiol. 24 (3), 1672–1686.

Darriba, D., Posada, D., Kozlov, A.M., Stamatakis, A., Morel, B., Flouri, T., 2020. ModelTest-NG: a new and scalable tool for the selection of DNA and protein evolutionary models. Mol. Biol. Evol. 37 (1), 291–294.

Dubuffet, A., Chauvet, M., Moné, A., Debroas, D., Lepère, C., 2021. A phylogenetic framework to investigate the microsporidian communities through metabarcoding and its application to lake ecosystems. Environ. Microbiol. 23 (8), 4344–4359.

Eddy, S.R., 2011. Accelerated profile HMM searches. PLoS Comput. Biol. 7 (10), e1002195.

Emms, D.M., Kelly, S., 2019. OrthoFinder: phylogenetic orthology inference for comparative genomics. Genome Biol. 20, 1–14.

Freeman, M.A., Turnbull, J.F., Yeomans, W.E., Bean, C.W., 2010. Prospects for management strategies of invasive crayfish populations with an emphasis on biological control. Aquat. Conserv. Mar. Freshwat. Ecosyst. 20, 211–223.

Frizzera, A., Bojko, J., Cremonte, F., Vázquez, N., 2021. Symbionts of invasive and native crabs, in Argentina: The most recently invaded area on the Southwestern Atlantic coastline. J. Invertebr. Pathol. 184, 107650.

Gurevich, A., Saveliev, V., Vyahhi, N., Tesler, G., 2013. QUAST: quality assessment tool for genome assemblies. Bioinformatics 29, 1072–1075.

Hyatt, D., Chen, G.L., LoCascio, P.F., Land, M.L., Larimer, F.W., Hauser, L.J., 2010. Prodigal: prokaryotic gene recognition and translation initiation site identification. BMC Bioinf. 11 (1), 1–11.

Jones, P., Binns, D., Chang, H.Y., Fraser, M., Li, W., McAnulla, C., Hunter, S., 2014. InterProScan 5: genome-scale protein function classification. Bioinformatics 30 (9), 1236–1240.

Karpov, S.A., Mamkaeva, M.A., Aleoshin, V.V., Nassonova, E., Lilje, O., Gleason, F.H., 2014. Morphology, phylogeny, and ecology of the aphelids (Aphelidea, Opisthokonta) and proposal for the new superphylum Opisthosporidia. Front. Microbiol. 5, 112.

Kozlov, A.M., Darriba, D., Flouri, T., Morel, B., Stamatakis, A., 2019. RAxML-NG: a fast, scalable and user-friendly tool for maximum likelihood phylogenetic inference. Bioinformatics 35 (21), 4453–4455.

Lange, C.E., Azzaro, F.G., 2008. New case of long-term persistence of *Paranosema locustae* (Microsporidia) in melanopline grasshoppers (Orthoptera: Acrididae: Melanoplinae) of Argentina. J. Invertebr. Pathol. 99 (3), 357–359.

Lipa, J.J., Tokarev, Y.S., Issi, I.V., 2020. Ultrastructure, molecular phylogeny, and prevalence rates of *Alternosema bostrichidis* gen. nov. sp. nov. (Microsporidia, Terresporidia), a parasite of *Prostephanus truncatus* and *Dinoderus* spp. (Coleoptera, Bostrichidae). Parasitol. Res., 119(3), 915–923.

Longshaw, M., 2011. Diseases of crayfish: A review. J. Invertebr. Pathol. 106, 54–70.

Menzel, P., Ng, K.L., Krogh, A., 2016. Fast and sensitive taxonomic classification for metagenomics with Kaiju. Nat. Commun. 7 (1), 11257.

Momot, W.T., 1995. Redefining the role of crayfish in aquatic ecosystems. Rev. Fish. Sci. 3, 3–63.

Moodie, E.G., Le Jambre, L.F., Katz, M.E., 2003a. *Thelohania montirivulorum* sp. nov. (Microspora: Thelohaniidae), a parasite of the Australian freshwater crayfish, *Cherax destructor* (Decapoda: Parastacidae): fine ultrastructure, molecular characteristics and phylogenetic relationships. Parasitol. Res. 91, 215–228.

Moodie, E.G., Le Jambre, L.F., Katz, M.E., 2003b. *Thelohania parastaci* sp. nov. (Microspora: Thelohaniidae), a parasite of the Australian freshwater crayfish, *Cherax destructor* (Decapoda: Parastacidae). Parasitol. Res. 91, 151–165.

Moodie, E.G., Le Jambre, L.F., Katz, M.E., 2003c. Ultrastructural characteristics and small subunit ribosomal DNA sequence of *Vairmorpha cheracis* sp. nov., (Microspora: Burenellidae), a parasite of the Australian yabby, *Cherax destructor* (Decapoda: Parastacidae). J. Invertebrate Pathol. 84, 198–213.

Murareanu, B.M., Sukhdeo, R., Qu, R., Jiang, J., Reinke, A.W., 2021. Generation of a microsporidia species attribute database and analysis of the extensive ecological and phenotypic diversity of microsporidia. MBio 12 (3) e01490-e0521.

Nishikori, K., Setiamarga, D.H., Tanji, T., Kuroda, E., Shiraishi, H., Ohashi-Kobayashi, A., 2018. A new microsporidium *Percutemincola moriokae* gen. nov., sp. nov. from *Oscheius tipulae*: A novel model of microsporidia–nematode associations. Parasitology 145 (14), 1853–1864.

Olden, J.D., McCarthy, J.M., Maxted, J.T., Fetzer, W.W., Vander Zanden, M.K., 2006. The rapid spread of rusty crayfish (*Orconectes rusticus*) with observations on native

crayfish declines in Wisconsin (U.S.A.) over the past 130 years. Biol. Invasions 8, 1621–1628.
Pretto, T., Montesi, F., Ghia, D., Berton, V., Abbadi, M., Gastaldelli, M., Manfrin, A., Fea, G., 2018. Ultrastructural and molecular characterization of *Vairimorpha austropotamobii* sp. nov. (Microsporidia: Burenellidae) and *Thelohania contejeani* (Microsporidia: Thelohaniidae), two parasites of the white-clawed crayfish, *Austropotamobius pallipes* complex (Decapoda: Astacidae). J. Invertebr. Pathol. 151, 59–75.
Rabeni, C.F., Gossett, M., McClendon, D.D., 1995. Contribution of crayfish to benthic invertebrate production and trophic ecology of an Ozark stream. Freshwater Crayfish. 10, 163–173.
Reinke, A.W., Balla, K.M., Bennett, E.J., Troemel, E.R., 2017. Identification of microsporidia host-exposed proteins reveals a repertoire of rapidly evolving proteins. Nat. Commun. 8 (1), 14023.
Schneider, C.A., Rasband, W.S., Eliceiri, K.W., 2012. NIH Image to ImageJ: 25 Years of Image Analysis. Nat. Methods 9, 671–675.
Seppey, M., Manni, M., Zdobnov, E.M., 2019. BUSCO: assessing genome assembly and annotation completeness. Gene Prediction: Methods Protocols 227–245.
Sokolova, Y.Y., Lange, C.E., Fuxa, J.R., 2006. Development, ultrastructure, natural occurrence, and molecular characterization of *Liebermannia patagonica* ng, n. sp., a microsporidian parasite of the grasshopper *Tristira magellanica* (Orthoptera: Tristiridae). J. Invertebr. Pathol. 91 (3), 168–182.
Sokolova, Y.Y., Lange, C.E., Fuxa, J.R., 2007. Establishment of *Liebermannia dichroplusae* n. comb. on the basis of molecular characterization of *Perezia dichroplusae* Lange, 1987 (Microsporidia). J. Eukaryot. Microbiol. 54 (3), 223–230.
Sokolova, Y., Pelin, A., Hawke, J., Corradi, N., 2015. Morphology and phylogeny of *Agmasoma penaei* (Microsporidia) from the type host, *Litopenaeus setiferus*, and the type locality, Louisiana, USA. Int. J. Parasitol. 45 (1), 1–16.
Stentiford, G.D., Bass, D., Williams, B.A., 2019. Ultimate opportunists—the emergent Enterocytozoon group microsporidia. PLoS Pathog. 15 (5), e1007668.
Stentiford, G.D., Bateman, K.S., Dubuffet, A., Chambers, E., Stone, D.M., 2011. *Hepatospora eriocheir* (Wang and Chen, 2007) gen. et comb. nov. infecting invasive Chinese mitten crabs (*Eriocheir sinensis*) in Europe, J. Invertebrate Pathol., 108 (3), 156–166.
Stratton, C.E., DiStefano, R.J., 2021. Is native crayfish conservation a priority for United States and Canadian fish and wildlife agencies? Freshwater Crayfish. 26, 25–26.
Stratton, C.E., Moler, P., Allain, T.W., Reisinger, L.S., Behringer, D.C., Bojko, J., 2022a. The plot thickens: *Ovipleistophora diplostomuri* infects two additional species of Florida crayfish. J. Invertebr. Pathol. 191, 107766.
Stratton, C.E., Reisinger, L.S., Behringer, D.C., Bojko, J., 2022b. Revising the freshwater *Thelohania* to *Astathelohania* gen. et comb. nov., and description of two new species. Microorganisms. 10 (3), 636.
Taylor, C.A., Schuster, G.A., Wylie, D., 2015. Field guide to crayfishes of the Midwest. Ill. Nat. Hist. Surv.
Tedersoo, L., Sánchez-Ramírez, S., Kõljalg, U., Bahram, M., Döring, M., Schigel, D., May, T., Ryberg, M., Abarenkov, K., 2018. High-Level classification of the Fungi and a tool for evolutionary ecological analyses. Fungal Divers. 90, 135–159.
Teufel, F., Almagro Armenteros, J.J., Johansen, A.R., Gíslason, M.H., Pihl, S.I., Tsirigos, K.D., Nielsen, H., 2022. SignalP 6.0 predicts all five types of signal peptides using protein language models. Nat. Biotechnol. 40 (7), 1023–1025.
Tokarev, Y.S., Huang, W.F., Solter, L.F., Malysh, J.M., Becnel, J.J., Vossbrinck, C.R., 2020. A formal redefinition of the genera *Nosema* and *Vairimorpha* (Microsporidia: Nosematidae) and reassignment of species based on molecular phylogenetics. J. Invertebr. Pathol. 169, 107279.
Trifinopoulos, J., Nguyen, L.T., von Haeseler, A., Minh, B.Q., 2016. W-IQ-TREE: a fast online phylogenetic tool for maximum likelihood analysis. Nucleic Acids Res. 44 (W1). W232-W235.
Vávra, J., Hyliš, M., Fiala, I., Nebesářová, J., 2016. *Globulispora mitoportans* ng, n. sp., (Opisthosporidia: Microsporidia) a microsporidian parasite of daphnids with unusual spore organization and prominent mitosome-like vesicles. J. Invertebr. Pathol. 135, 43–52.
Vossbrinck, C.R., Baker, M.D., Didier, E.S., Debrunner-Vossbrinck, B.A., Shadduck, J.A., 1993. Ribosomal DNA sequences of *Encephalitozoon hellem* and *Encephalitozoon cuniculi*: species identification and phylogenetic construction. J. Eukaryot. Microbiol. 40, 354–362.
Vossbrinck, C.R., Debrunner-Vossbrinck, B.A.,Weiss, L.M., 2014. Phylogeny of the Microsporidia. Pathogens of Opportunity, Microsporidia, pp. 203–220.
Wadi, L., El Jarkass, H.T., Tran, T.D., Islah, N., Luallen, R.J., Reinke, A.W., 2022. Genomic and phenotypic evolution of nematode-infecting microsporidia. bioRxiv. 2022-08.
Wickham, H., 2011. ggplot2. Wiley Interdiscip. Rev. Comput. Stat. 3 (2), 180–185.
Wijayawardene, N.N., Hyde, K.D., Al-Ani, L.K.T., Tedersoo, L., Haelewaters, D., Rajeshkumar, K.C., Deng, C., 2020. Outline of Fungi and fungus-like taxa. Mycosphere 11 (1), 1060–1456.
Wiredu Boakye, D., Jaroenlak, P., Prachumwat, A., Williams, T.A., Bateman, K.S., Itsathitphaisarn, O., Williams, B.A., 2017. Decay of the glycolytic pathway and adaptation to intranuclear parasitism within Enterocytozoonidae microsporidia. Environ. Microbiol. 19 (5), 2077–2089.
Zhang, G., Sachse, M., Prevost, M.C., Luallen, R.J., Troemel, E.R., Felix, M.A., 2016. A large collection of novel nematode-infecting microsporidia and their diverse interactions with *Caenorhabditis elegans* and other related nematodes. PLoS Pathog. 12 (12), e1006093.